1997

Parametric Kinematic Tolerance Analysis of General Planar Systems

Elisha Sacks
Purdue University, eps@cs.purdue.edu

Leo Joskowicz

Report Number:
97-027

PARAMETRIC KINEMATIC TOLERANCE ANALYSIS OF GENERAL PLANAR SYSTEMS

Elisha Sacks
Leo Joskowicz

CSD-TR #97-027
May 1997
(Revised March 1998)
(NOTE: TITLE CHANGE)

Parametric kinematic tolerance analysis of general planar systems

Elisha Sacks
Computer Science Department
Purdue University
West Lafayette, IN 47907, USA
E-mail: eps@cs.purdue.edu

Leo Joskowicz
Institute of Computer Science
The Hebrew University
Jerusalem 91904, Israel
E-mail: josko@cs.huji.ac.il

March 18, 1998

Abstract

We present an algorithm for functional kinematic tolerance analysis of general planar mechanical systems with parametric tolerances. The algorithm performs worst-case analysis of systems of curved parts with contact changes, including open and closed kinematic chains. It computes quantitative variations and helps designers detect qualitative variations, such as blocking and under-cutting. The algorithm constructs a variation model for each interacting pair of parts: a mapping from the part tolerances and configurations to the kinematic variation of the pair. These models generalize the configuration space representation of nominal kinematics to toleranced parts. They are composed via sensitivity analysis and linear programming to derive the system variation at a given configuration. The variation relative to the nominal system function is computed by sampling the system variation. We demonstrate the algorithm on detailed parametric models of a movie camera film advance and of a micro-mechanical gear discriminator.

Keywords: functional tolerance analysis, contact analysis, kinematic variation.

Submitted, *Computer-Aided Design*, March 1998.

1 Introduction

We present an algorithm for functional kinematic tolerance analysis of general planar mechanical systems with parametric tolerances. Tolerance analysis is the task of determining the effects of manufacturing variation on product performance and quality. Designers use tolerance analysis to create products that are reliable, economical, and easy to assemble. Tolerancing bridges the gap between design and manufacturing. It is an integral part of the product design process with far-reaching economic consequences. The complexity, diversity, and short design cycle of modern products increases the need for computer-assisted tolerancing as part of computer-aided design. Commercial systems address some aspects of tolerancing, but they are restricted in scope and most tasks still fall on the designer. Research in computer-assisted tolerancing aims to remedy this situation.

Tolerance analysis consists of tolerance specification, variation modeling, and sensitivity analysis. Tolerance specification defines the allowable variation in the shapes and configurations of the parts of a system. The most common are parametric and geometric tolerance specifications [25, 18]. Variation modeling produces mathematical models that map tolerance specifications to assembly and function variations. Sensitivity analysis estimates the worst-case and statistical variations of critical properties in the model for given part variations. Designers iterate through these steps to synthesize optimal tolerance allocations relative to their cost criteria.

The goals of mechanical systems tolerancing are to produce designs that can be assembled and that function correctly despite manufacturing variation. In assembly tolerancing, very general part variations must be modeled, so geometric tolerance specifications are most frequently used. Statistical sensitivity analysis is most common because guaranteed assembly is more expensive than discarding a few defective products. Most algorithms perform tolerance analysis on the final assembled configuration [3], although recent research explores toleranced assembly sequencing [13]. In functional tolerancing, the relevant part variations occur in functional features whose description is parametric. Parametric tolerances, which are simpler than geometric tolerances, are best suited to capture these variations. Worst-case analysis is most appropriate because functional failures that occur after product delivery can be extremely expensive.

Our research addresses functional kinematic tolerance analysis of mechanical systems. This is the most important form of functional tolerance analysis because kinematic function, which is described by motion constraints due to part contacts, largely determines mechanical system function. The task is to compute the variation in the part motions due to variations in the tolerance parameters. For example, variation in the gear profiles and rotation axes of a transmission causes backlash and transmission ratio variation. Variation modeling derives the functional relationship between the tolerance parameters and the system kinematic function. Sensitivity analysis determines the variation of this function over the allowable parameter values.

Creating a variation model is the limiting factor in kinematic tolerance analysis. The analyst has to formulate and solve large systems of algebraic equations to obtain the relationship between the tolerance parameters and the kinematic function. The analysis grows much harder when we consider systems with contact changes. Contact changes occur in the nominal function of higher pairs, such as gears, cams, clutches, and ratchets. Part variation produces contact changes in systems whose nominal designs prescribe permanent contacts. The analysis has to determine which contacts occur at each stage of the work cycle, to derive the resulting kinematic functions, and to identify qualitative kinematic variations due to contact changes, such as play, under-cutting, interference, and jamming. Once the variation model is obtained, sensitivity analysis can be performed by linearization, statistical analysis, or Monte Carlo simulation [3].

We present a functional kinematic tolerance analysis algorithm for general planar systems with lower and higher pairs, open and closed kinematic chains, and contact changes. The algorithm computes worst-case variations and helps designers detect qualitative effects of part variations on kinematic function. It constructs a variation model from the nominal part geometry and the tolerance specifications then performs sensitivity analysis. It analyzes systems with 50 to 100 parameters in a few minutes, which permits interactive tolerancing of detailed functional models.

The rest of the paper is organized as follows. The next section contains a review of previous work on kinematic tolerance analysis. The following section describes our configuration space representation of nominal kinematic function. In the following two sections, we present a kinematic tolerance analysis algorithm for planar pairs based upon an extension of configuration space to toleranced parts. In the following section, we extend the algorithm to planar systems. We demonstrate the algorithm on a movie camera film advance and on micro-mechanical gear discriminator. We conclude with directions for future work.

2 Previous work

Previous work on kinematic tolerance analysis of mechanical systems falls into three, increasingly general categories: static (small displacement) analysis, kinematic (large displacement) analysis of fixed contact systems, and kinematic analysis of systems with contact changes. Static analysis of fixed contacts, also referred to as tolerance chain or stack-up analysis, is the most common. It consists of identifying a critical dimensional parameter (a gap, clearance, or play), building a tolerance chain based on part configurations and contacts, and determining the parameter variability range using vectors, torsors, or matrix transforms [4, 26]. Recent research explores static analysis with contact changes [9, 1]. Kinematic analysis of fixed contact mechanical systems, such as linkages, has been thoroughly studied in mechanical engineering [6]. It consists of defining kinematic relations between parts and studying their kinematic variation [2]. Most commercial CAT systems include this capability for planar

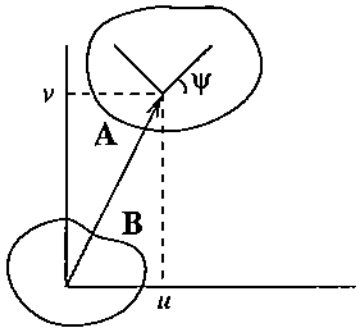

Figure 1: Generic configuration space for planar pairs.

and spatial mechanism [24].

Our previous work addresses kinematic analysis with contact changes in planar system whose parts move along fixed axes [23]. Based on the configuration space representation of kinematic function, we developed an algorithm that computes variation models of the interacting pairs of parts and composes them to derive the system variation. The algorithm performs worst-case and statistical analysis. The main shortcoming of the variation models is their inability to express part play: parts with one nominal degree of freedom that acquire additional degrees of freedom due to imperfect joints. The main limitation of the composition algorithm is that it cannot model closed chains, which are common when parts have three degree of freedom.

Our new algorithm eliminates both restrictions. It uses generalized three-dimensional configuration spaces to model kinematic variation in general planar pairs. It handles closed chains by solving systems of linearized variation equations.

3 Configuration space

We model kinematic function within the configuration space representation of rigid body interaction [10, 21]. Configuration space is a general representation for systems of rigid parts that is widely used in robot motion planning [16, 12]. We model the interactions of pairs of planar parts with three-dimensional spaces whose points specify the spatial configuration (position and orientation) of one part with respect to the other (Figure 1).

Configuration space partitions into three disjoint sets that characterize part interaction: blocked space where the parts overlap, free space where they do not touch, and contact space where they touch without overlap. Blocked space represents unrealizable configurations, free space represents independent part motions, and contact space represents motion constraints due to part contacts. (Latombe [12] provides formal set theoretic definitions). The spaces have useful topological properties. Free and blocked space are open sets whose common boundary is contact space. Contact space is a closed set comprised of algebraic patches that

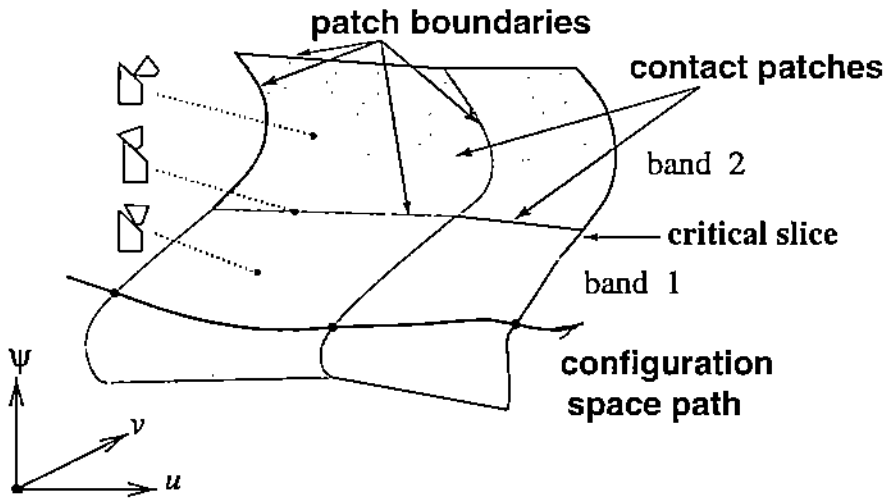

Figure 2: Illustration of contact space. Part contacts on the left show typical contact configurations.

represent contacts between pairs of part features. Patch boundary curves represent simultaneous contacts between two pairs of part features. As the parts move, their configurations trace a curve through free and contact space (Fig. 2). Contact changes occur when the curve crosses patch boundaries.

The film advance of a movie camera illustrates these concepts (Figure 3). The driver cam rotates about a shaft on the frame, while the enclosing follower is attached to the frame by a pin joint. The film translates vertically in a plane orthogonal to the page. As the cam rotates counter-clockwise, the follower tip engages the film, pushes it down one frame, and retracts. The driver coordinate frame is at the center of the shaft, while the follower frame is at the center of the square opening. Figure 4a shows the $\psi = 0.6$ radians cross-section of the driver/follower configuration space, which represents part translations at the displayed orientations. The contact space is a square formed by four contact curves (lines in this case) corresponding to the four possible contacts between pairs of cam and follower features. For example, the top of the square represents contacts between the top arc of the cam and the top of the follower inner profile. The free space represents cam play: it delimits the cam translations at the given orientation. The other configuration space slices have the same shape, since the cam has constant breadth, but are shifted horizontally and vertically. Figure 4b shows the three-dimensional configuration space. The free space forms a narrow spiral channel bounded by the contact patches. The blocked space is the exterior of the channel.

We have developed a configuration space computation program for planar pairs whose part boundaries consist of line segments and circular arcs [19, 21]. These features suffice for most engineering applications with the exception of involute gears and precision cams,

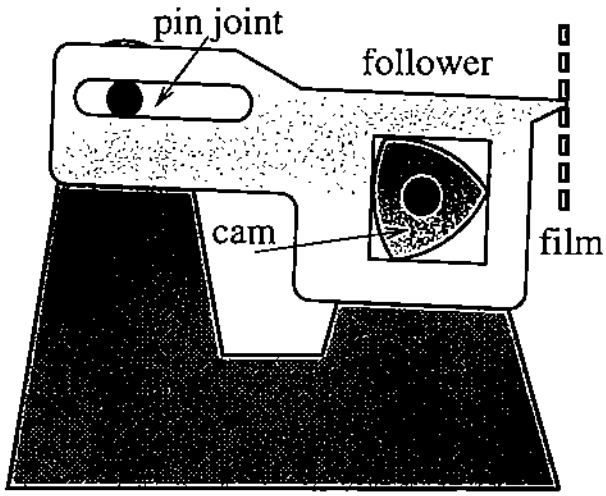

Figure 3: Film advance mechanism of a movie camera.

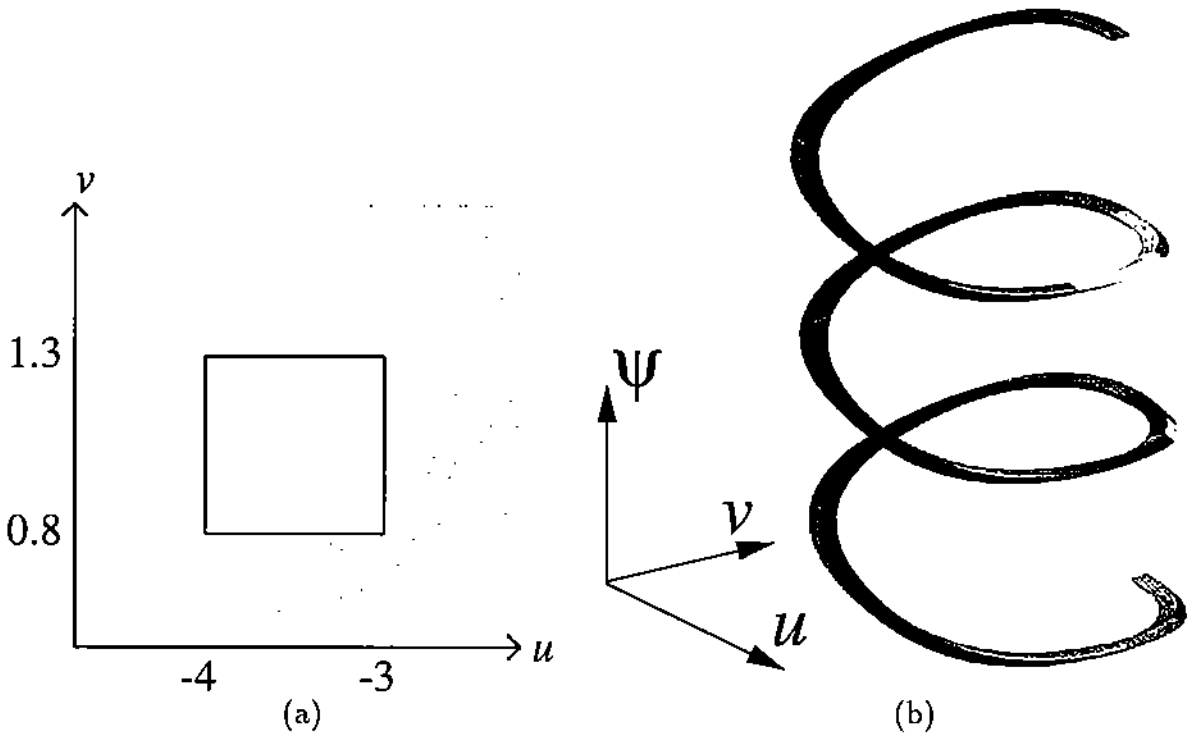

Figure 4: (a) Driver/follower configuration space slice for orientation $\psi = 0.6$ radians. (b) Three-dimensional contact space for $-\pi \leq \psi \leq \pi$. Contact patches are shaded. The uv scale is millimeters.

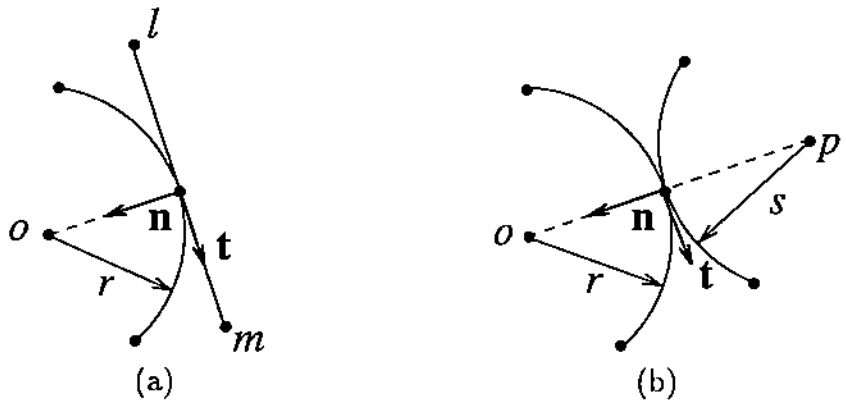

Figure 5: Planar feature contacts: (a) contact between a circular arc and a line segment, and (b) contact between two circular arcs. Shading indicates part interior.

which are best handled by specialized methods [8, 15]. The program computes an exact representation of contact space: a graph whose nodes represent contact patches and whose arcs represent patch adjacencies. Each node contains a contact function that evaluates to zero on the patch, is positive in nearby free configurations, and is negative in nearby blocked configurations. Each graph arc contains a parametric representation of the boundary curve between its incident patches. We summarize the details that are relevant to this paper.

There are three types of contact patches, corresponding to the types of features in contacts: moving arc/fixed line, moving line/fixed arc, and moving arc/fixed arc. Contacts involving points are identical to those for arcs of radius zero. Line/line contacts are subsumed by line/point contacts. Figure 5a shows an arc/line contact. The contact condition is that the distance between the center o of the arc and the line lm equals the arc radius r:

$$(\mathbf{o} - \mathbf{l}) \times (\mathbf{m} - \mathbf{l}) = dr \tag{1}$$

where $\times$ denotes the vector cross-product, d is the length of the line segment, and its interior lies to the left when traversed from l to m. Figure 5b shows an arc/arc contact. The contact condition is that the distance between the centers equals the sum of the radii:

$$(\mathbf{o} - \mathbf{p}) \cdot (\mathbf{o} - \mathbf{p}) \;\; = \;\; (r + s)^2$$

where r and s are positive for convex arcs and negative for concave arcs.

We obtain the contact patch functions from these equations by expressing points in coordinates. The coordinates of a point on the fixed part are $\mathbf{q} = (q_x, q_y)$. The coordinates of a moving point are $\mathbf{p} = (u, v) + R_\psi(p_x, p_y)$ with (p_x, p_y) the part coordinates and with R_ψ a rotation matrix. We obtain functions of the form $g(u, v, \psi) = 0$ that are parameterized by the part features. The moving arc/fixed line function is

$$u(m_y - l_y) - v(m_x - l_x) + (m_y - l_y)(o_x \cos\psi - o_y \sin\psi) - (m_x - l_x)(o_x \sin\psi + o_y \cos\psi) = dr. \tag{2}$$

The moving line/fixed arc equation is

$$(u-o_x)(l_x\cos\psi-l_y\sin\psi)-(v-o_y)(l_x\sin\psi+l_y\cos\psi)+l_x(m_y-l_y)-l_y(m_x-l_x)+dr=0. \quad (3)$$

The moving arc/fixed arc equation is

$$u^2+v^2+2(o_x\cos\psi-o_y\sin\psi)u+2(o_x\sin\psi+o_y\cos\psi)v+o_x^2+o_y^2+p_x^2+p_y^2-(r+s)^2=0. \quad (4)$$

After constructing configuration spaces for the kinematic pairs in a mechanical system, we analyze the system mechanical function in the system configuration space. We use a $3n$-dimensional configuration space whose coordinates specify the n part configurations relative to a global coordinate frame. These coordinates are related to the relative coordinates of the pairs by the equations

$$\begin{aligned} u &= \cos\theta_B(x_A-x_B)+\sin\theta_B(y_A-y_B) \\ v &= \cos\theta_B(y_A-y_B)-\sin\theta_B(x_A-x_B) \\ \psi &= \theta_A-\theta_B. \end{aligned} \quad (5)$$

where (x_A, y_A, θ_A) and (x_B, y_B, θ_B) denote the configurations of parts A and B in the global coordinate frame. A system configuration is free when no parts touch, is blocked when two parts overlap, and is in contact when two parts touch and no parts overlap. We construct the relevant portion of the system configuration space from the pairwise spaces.

4 Kinematic variation in pairs

We model kinematic variation by generalizing the configuration space representation to toleranced parts. The contact patches of a pair are parameterized by the touching features, which depend on the tolerance parameters. As the parameters vary around their nominal values, the contact patches vary in a band around the nominal contact space, which we call the contact zone [11]. For example, Figure 6 shows a cross-section of the cam/follower contact zone, which forms a narrow envelope around the three-dimensional configuration space in Figure 4. The contact zone defines the kinematic variation in each contact configuration: every pair that satisfies the part tolerances generates a contact space that lies in the contact zone. Kinematic variations do not occur in free configurations because the parts do not interact.

Each contact patch generates a region in the contact zone that represents the kinematic variation in the corresponding feature contact. The region boundaries encode the worst-case kinematic variation over the allowable parameter variations. They are smooth functions of the tolerance parameters and of the part configurations in each region. They are typically discontinuous at patch boundaries because the adjacent patches depend on different parameters. The variation at boundary configurations is the maximum over the neighboring patch

variations. The contact zone regions represent the quantitative kinematic variation, while the relations among regions represent qualitative variations such as jamming, under-cutting, and interference.

We illustrate these concepts on a parametric model of the cam/follower pair. The cam has a nominal breath of 30 mm and the nominal follower profile is a is 30.5 mm side square, so the nominal clearance is 0.5 mm. The cam tolerance model has 12 functional parameters: the cam breadth, the horizontal and vertical offsets of the rotation axis, and two endpoint coordinates and one radius per arc. The follower tolerance model has 11 functional parameters: the horizontal, vertical, and angular position of the follower, and the two coordinates of the four corners of the follower profile. The pin/slot contact is modeled as a lower pair. The tolerance parameters represent variations from the nominal values of functional parameters, hence are zero in the nominal system.

Figure 6a shows the contact zone for symmetric tolerance intervals of 0.01 mm on all 23 parameters. The contact zone is a narrow band around the nominal contact curves. The outer boundary shows the largest possible clearance, while the inner boundary shows the smallest clearance. The variation in horizontal clearance, which is the distance between the inner and outer verticals, is 0.05 mm, while the variation in vertical clearance is 0.08mm. As the tolerance grows, the maximum clearance (outer rectangle) grows and the minimum clearance (inner rectangle) shrinks. At a certain point, the minimum clearance becomes zero and beyond that certain cam instances do not fit into the follower. This is illustrated in Figure 6b where a tolerance of 0.07 mm shrinks the inner rectangle until the vertical lines a and b cross each other.

5 Contact zone computation

We compute the contact zone from the parametric part models and the nominal contact patches. Each patch satisfies a contact equation $g(u, v, \psi) = 0$, which we rewrite as $g(u, v, \psi, \mathbf{p}) = 0$ to make explicit the dependence on the vector $\mathbf{p}$ of tolerance parameters. The configuration space computation program forms these functions by substituting the parametric expressions for the part features into Equations 2–4. A parameter perturbation of $\delta\mathbf{p}$ leads to a perturbed patch that satisfies

$$g(u + \delta u, v + \delta v, \psi + \delta\psi, \mathbf{p} + \delta\mathbf{p}) = 0. \tag{6}$$

Following the standard tolerancing approximation which considers only the first-order effects on kinematic variation, we obtain the linear expression

$$\frac{\partial g}{\partial u}\delta u + \frac{\partial g}{\partial v}\delta v + \frac{\partial g}{\partial \psi}\delta\psi = -\sum_i \frac{\partial g}{\partial p_i}\delta p_i \tag{7}$$

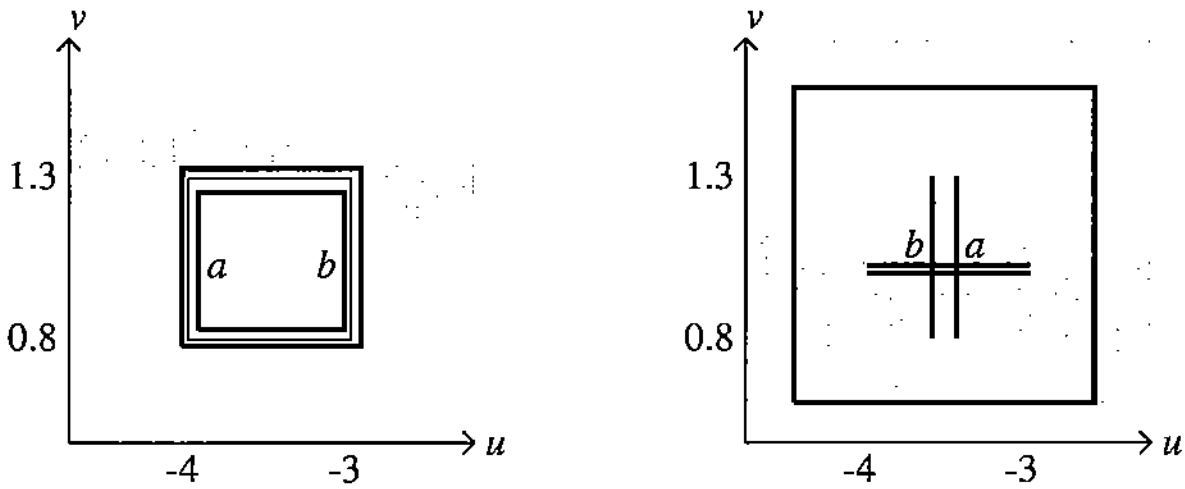

Figure 6: Cross sections at orientation $\psi = 0.6$ radians of the cam/follower nominal contact space (thin line) and contact zones (thick lines) for two tolerance intervals. Shading indicates blocked nominal configurations.

where the partial derivatives of g are evaluated at (u, v, ψ) and δp_i is the ith element of δp. This equation approximates the portion of the perturbed patch near the configuration (u, v, ψ) with a plane.

The left side of Equation 7 specifies the normal direction of the perturbed contact patch, which is independent of the parameter variations. The right side specifies the distance between the perturbed and the nominal patch, that is the kinematic variation, for any allowable parameter variation $l_i \leq \delta p_i \leq u_i$ with $l_i \leq 0$ and $u_i \geq 0$. The worst-case kinematic variation (largest distance) occurs when the right side is maximal or minimal. It is maximal when every term is maximal, which occurs when $\delta p_i = l_i$ when $g_{p_i} > 0$ and $\delta p_i = u_i$ otherwise. Switching u_i and l_i yields the minimal value.

We compute cross-sections of the perturbed patch at user-specified ψ values. The cross-sections can be examined individually, as in the cam/follower example, or can be triangulated to approximate the perturbed patch. Each cross-section is represented by a sequence of points. The nominal points are obtained by discretizing the nominal contact curve to a user-specified accuracy. The perturbed points are found by setting $\delta v = 0$ and $\delta\psi = 0$ in Equation 7 and solving for δu, which is a vertical offset from the nominal curve. If the nominal curve is vertical, δu and δv trade roles to yield a horizontal offset. In the film advance example, we chose a ψ spacing of 0.1 radians and a 0.001 mm spacing for u and v. The cross sections are horizontally and vertically shifted versions of the ones in Figure 6.

6 Kinematic variation in systems

The contact zone model of worst-case kinematic variation generalizes from pairs to systems. The contact space is a semi-algebraic set in configuration space: a collection of points, curves, surfaces, and higher dimensional components. As the tolerance parameters vary around their nominal values, the components vary in a band around the nominal contact space, which is a higher-dimensional analog of the three-dimensional contact zone of a pair. We could in principle compute these contact zones by general algebraic methods [12] or by linearization [10], but these are impractical for all but the simplest inputs. We avoid this computational roadblock by performing kinematic tolerance analysis on individual operating modes.

System operating modes are defined by driving forces and initial conditions. For example, the forward operating mode of the movie camera film advance occurs when a motor applies a constant counter-clockwise torque to the driving cam, while the reverse mode occurs when the torque is applied clockwise. We can perform the analysis for any number of modes, but cannot analyze the sensitivity to the continuously infinite space of all possible modes. Given the forces and initial conditions, the laws of physics determine the time evolution of the system state (part configurations and velocities). We can compute a nominal sequence of states by kinematic simulation [20], by dynamical simulation [22] or by physical measurement. This yields a nominal path in the system configuration space. We perform kinematic tolerance analysis by computing the kinematic variation at sampled configurations along the nominal path.

We compute the system variation at each configuration along the nominal path by determining which pairs of parts are in contact, obtaining the corresponding parameterized contact equations from the pairwise configuration spaces, and solving a linear optimization problem. The variables are the part coordinate variations $(\delta x_i, \delta y_i, \delta\theta_i)$ and the tolerance parameters p_i. The constraints come from the tolerances and from the contact patches. The tolerances provide two constraints per parameter $l_i \leq p_i \leq u_i$. We collect the contact equations into a vector equation

$$\mathbf{g}(\mathbf{x}, \mathbf{p}) = 0 \tag{8}$$

with $\mathbf{x}$ the part coordinates and $\mathbf{p}$ the tolerance parameters. We linearize the contact equations around the current configuration and the nominal parameter values to obtain

$$D_{\mathbf{x}}\mathbf{g}\delta\mathbf{x} + D_{\mathbf{p}}\mathbf{g}\delta\mathbf{p} = 0 \tag{9}$$

with $D_{\mathbf{x}}\mathbf{g}$ the Jacobian matrix with respect to $\mathbf{x}$ and $D_{\mathbf{p}}\mathbf{f}$ the Jacobian matrix with respect to $\mathbf{p}$. This equation is the system analog of Equation 7. It approximates the portion of the perturbed configuration space near $\mathbf{x}$ with a hyper-plane. The objective functions are the maxima and minima of the coordinate variations. We solve one linear program for each function to obtain the system variation.

The kinematic variation represents a worst-case value relative to the unknown values of the internal degrees of freedom of the system. Some are governed by driving motions, such

as the cam orientation in the film advance. Others represent part play: small motions that are absent from the nominal system, but arise the toleranced system due to imperfect joints. The remaining degrees of freedom are governed by dynamical effects, such as gravity, springs, and friction. To tighten the worst-case bounds on the kinematic variation, we augment the linear program with constraints for driving motions and for part play. Dynamical degrees of freedom are a topic for future research, as discussed in the conclusions.

Driving motions give rise constraints of the type $\delta x_i = 0$, which indicates that the part coordinate x_i equals its nominal value. These constraints uniquely determine the kinematic variation in systems that have as many driving motions as degrees of freedom, which is the norm. We model part play as range constraints on part coordinates. For example, a pin joint with one unit of clearance gives rise to the constraints $-1 \leq \delta u \leq 1$ and $-1 \leq \delta v \leq 1$ on the relative horizontal and vertical position of the attached parts. We could readily replace the range constraints with general linear constraints. Nonlinear constraints are also useful, but probably not worth the computational cost of solving the resulting nonlinear optimization problems. For example, a more accurate pin joint constraint is $\delta u^2 + \delta v^2 = 1$, but the range constraint is normally fine and a polyhedral approximation is very good.

7 Results

We have implemented the kinematic tolerance analysis algorithms for planar pairs and for general planar systems. We illustrate the algorithms on the film advance mechanism and on a micro-mechanism.

7.1 Film advance

The film advance mechanism has three moving parts and between seven and nine contact constraints. The frame/cam and frame/film joints each provide two constraints, the frame/follower provides one, and the follower/film provides one. The cam/follower provides between one and three simultaneous contacts. The double contact is designed to move the follower along the correct motion path. The single contact is a consequence of the follower play in the nominal design, without which any part variation would cause jamming. The rare case of the triple contact occurs at transitions between double contacts. The mechanism has two degrees of freedom with a single contact, one in with two simultaneous contacts, and none with three simultaneous contacts.

We simulated one counter-clockwise rotation of the driver and obtained 393 configurations with a relative accuracy of 0.1%. The driver x, y and the follower y coordinates have zero variation because of their contacts with the frame, while the driver θ has zero variation because it is the driving motion. Hence, variations occur only in the follower y and θ coordinates. We imposed the bounds $-0.25mm \leq y \leq 0.25mm$, which represent the follower

nominal play.

The function of the follower is to push down the film one frame at a time. We computed the variation in the tip position throughout the work cycle. The nominal tip position is

$$\begin{bmatrix} t_x \\ t_y \end{bmatrix} = \begin{bmatrix} x \\ y \end{bmatrix} + R_\theta \begin{bmatrix} 28 \\ 2 \end{bmatrix} \tag{10}$$

with $(28, 2)$ mm the tip part coordinates and x, y, θ the follower configuration. We linearized this function to compute the variations δt_x and δt_y. We considered a symmetric tolerance interval of 0.01 mm on all parameters in two modes: the tip pushing down the film (engaged mode) and the tip retracted with the film stationary (disengaged mode). In the engaged mode, the variations are $0.03 \leq \delta t_x \leq 0.06$ mm and $0.03 \leq \delta t_y \leq 0.12$ mm. This deviation is too small to effect the function because the tip engages the film with a horizontal penetration of 5.0 mm and the vertical gap between film teeth is 4 mm. In the disengaged more, $0.25 \leq \delta t_x \leq 0.36$ mm and $0.07 \leq \delta t_y \leq 3.13$ mm, which is much larger than before but still does not affect the function. The large difference between the modes is due to the presence of one cam/follower contact in the disengaged mode versus two in the engaged mode. Moving the film plane horizontally 1 mm closer to the follower tip creates single contacts in the engaged mode that can cause mechanism failure on some part instances.

7.2 Micro-mechanism example

The second example is a micro-mechanical gear discriminator mechanism developed at Sandia National Laboratory (Figure 7). Micro-mechanical fabrication is a new technology that poses unique challenges for kinematic tolerancing and for computer-aided design in general. The part sizes range from tens to hundreds of microns. The shapes are accurate to 0.1 microns. Joints clearances are about one micron, which is very large relative to part size. If the parts that form the joint are closer, the fabrication process will fuse them.

We illustrate kinematic tolerance analysis on the indexing assembly whose function is to advance the gear by one tooth per pinion rotation (Figure 7b). The parts are a pinion, a gear, a pawl, and an anchor. The pinion drives the gear. The pawl prevents reverse rotation by blocking against the anchor. The design goal is to ensure this function despite part play.

In the ideal design, the pinion and gear have one degree of freedom apiece, so the configuration space is two-dimensional (Figure 8). This is *not* a cross-section of a three-dimensional configuration space because the coordinates are the two part orientations. The narrow diagonal channels represent coupled motion in which the pinion advances the gear, while the free space above represents the pinion rotating independently between gear engagements. Part tolerances create contact zones around the channels. The zones do not overlap for parameter tolerances of 0.1 microns, which shows that the nominal function is preserved.

Joint play gives each part two translational degrees of freedom, making the actual configuration space three-dimensional. Figure 9 shows two representative cross-sections of the

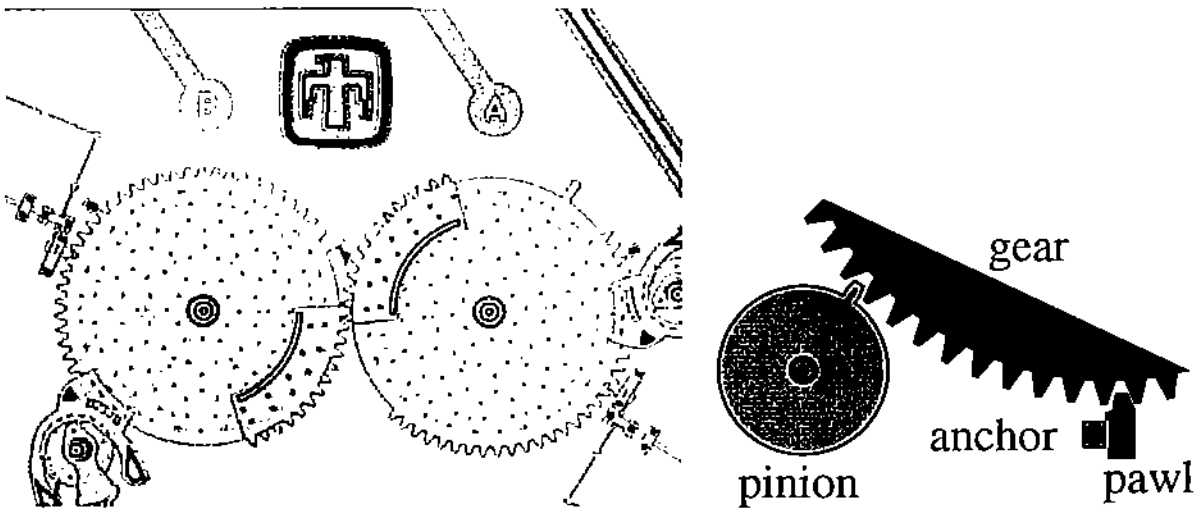

Figure 7: (a) Photograph of the micro-mechanical discriminator mechanism. The real size is about 200 microns; (b) detail of the indexing assembly CAD model.

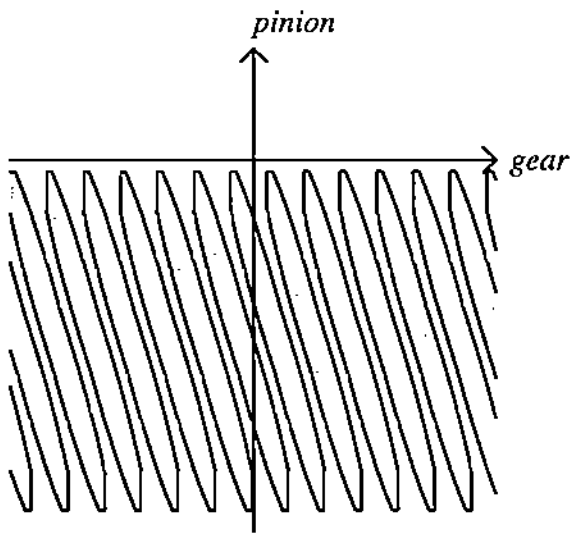

Figure 8: Configuration space for pinion/gear pair without play.

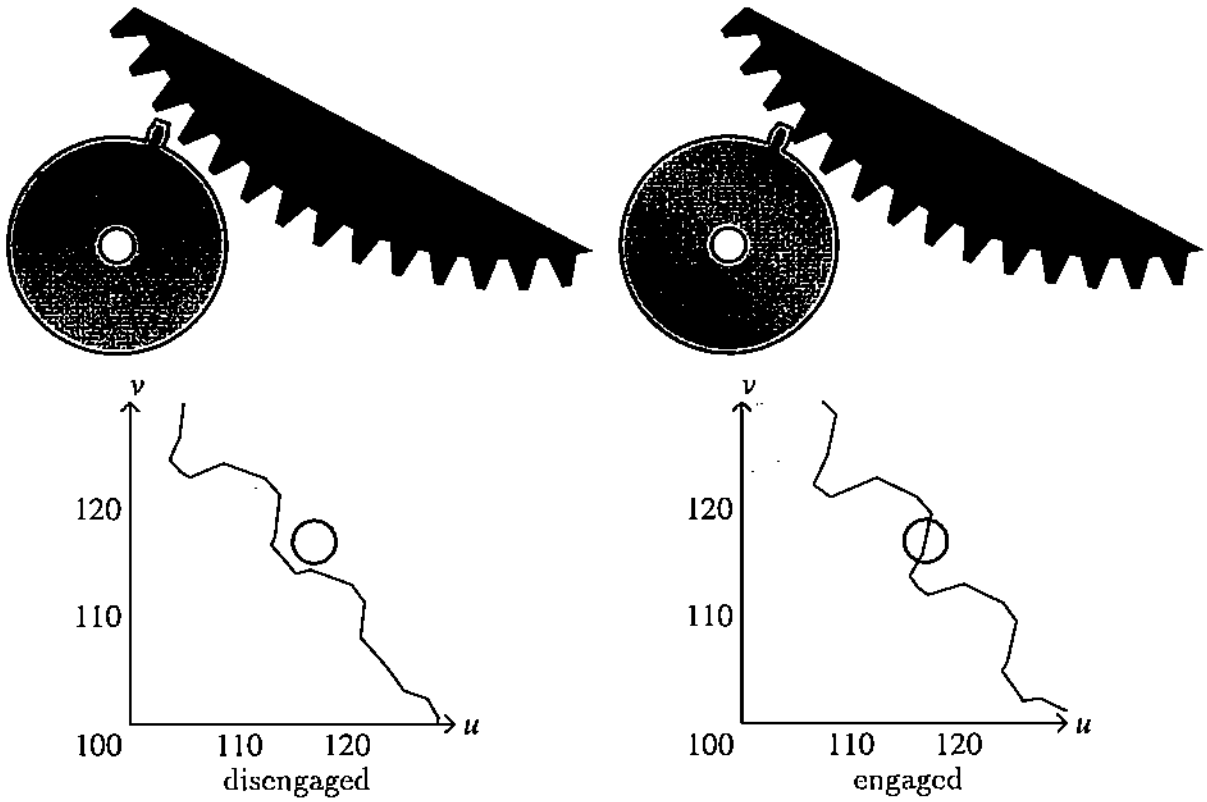

Figure 9: Cross-sections of the three-dimensional gear/pinion configuration space.

gear/pinion configuration space. The circles mark the range of motion due to joint play. The part play is too small to cause unintended contacts. In the disengaged orientation, the circle lies wholly in free space, which rules out other contacts that could cause chatter, vibration, and wear. In the engaged configuration, the circle center lies on the nominal contact curve and the circle does not intersect any other contact curves, which rules out backlash and jamming. We omit the figure of the full configuration, which consists of some 250,000 patches, because it is very hard to understand.

The next step in analyzing the indexing function is to test if quantitative kinematic variation can create failure modes. We answered this question by computing the kinematic variation along the nominal motion path. The system has nine part coordinates and two contact constraints. We imposed the bounds $-1 \leq x_g, y_g, x_p, y_p \leq 1$ on the translational coordinates (x_g, y_g) of the gear and (x_p, y_p) of the pinion. This is a conservative linear approximation of the 1 micron play, which imposes circle constraints $x_g^2 + y_g^2 = 1$ and $x_p^2 + y_p^2 = 1$, as discussed in the previous section. We picked the pinion orientation as the driving motion and computed the variation in the gear orientation over the drive phase.

We simulated one rotation of the pinion and obtained 310 configurations with an accuracy

of 0.001 micron per linear coordinate and 0.001 radian per orientation. The drive phase consists of 185 of these configurations. The kinematic variation in the gear orientation ranges from 0.01 radians to 0.011 radians. This variation does not endanger the indexing function because each gear tooth spans 0.1 radians, hence is perturbed by at most 10% due to joint clearance. We did not compute the kinematic variation due to part shape variation because it is an order of magnitude smaller than the clearance, hence inconsequential.

8 Conclusion

We have presented an algorithm for functional kinematic tolerance analysis of planar systems with parametric tolerances. The algorithm performs worst-case analysis and handles open and closed chains of curved parts with contact changes. Given the nominal part motions, parametric part models, and bounds on the parameter variations, the algorithm computes the worst-case pairwise and system variation at many sampled nominal configurations. It also detects qualitative variations, such as under-cutting, interference, and jamming. We demonstrated the algorithm on two detailed functional models.

The main advantages of our configuration space method are that it automates the contact analysis of all planar systems and that it captures quantitative and qualitative kinematic variations. The algorithm presented in this paper is an extension of our previous algorithm, which handles open-chain mechanisms whose parts move along fixed spatial axes. The key extensions are a three-dimensional configuration space computation algorithm and a general method of composing pairwise kinematic variations.

We plan to use our algorithm to study kinematic variation in systems whose joints are modeled as higher pairs. This will eliminate the current restriction to parametric variations on lower pair kinematics, such as link length variation, and other simplified models. We also plan to study spatial tolerancing of planar systems and tolerance synthesis.

Dynamical tolerance analysis is another important research project. Previous research has studied the dynamical effects of fixed part variations [5]. We aim to generalize the analysis to parametric families of part variations. Dynamical degrees of freedom can be modeled by augmenting Equation 9 with dynamical constraints on the part motions. One can formulate the dynamical equations of motion, integrate them numerically, and differentiate the trajectory with respect to the tolerance parameters using the variational equation method [17]. This analysis would also show the dynamical effects of part play, such as impacts, which are not captured by the constraint approach. Dynamical tolerancing is a topic for future research because the variational method needs to be extended to handle contact changes, which create discontinuities in the equations.

We plan to develop tolerance synthesis software based on our configuration space method of tolerance analysis. We envision a system where designers specify part geometry, tolerance parameters, and design goals, while the program proposes tolerance intervals.

Acknowledgments

Sacks is supported in part by NSF grants CCR-9617600 and CCR-9505745 and by the Purdue Center for Computational Image Analysis and Scientific Visualization. Joskowicz is supported in part by a grant from the Authority for Research and Development, The Hebrew University and by a Guastalla Faculty Fellowship, Israel. Jorg Peters helped generate the three-dimensional configuration space images.

References

[1] Ballot, E. and Bourdet, P. A computation method for the consequences of geometric errors in mechanisms. in: *Proc. of the 5th CIRP Int. Seminar on Computer-Aided Tolerancing*, 1997.

[2] Chase, K., Magleby, S., and Glancy, C. A comprehensive system for computer-aided tolerance analysis of 2d and 3d mechanical assemblies. in: *Proc. of the 5th CIRP Int. Seminar on Computer-Aided Tolerancing*, 1997.

[3] Chase, K. W. and Parkinson, A. R. A survey of research in the application of tolerance analysis to the design of mechanical assemblies. *Research in Engineering Design* **3** (1991) 23–37.

[4] Clément, A., Rivière, A., Serré, P., et al. The ttrs: 13 constraints for dimensioning and tolerancing. in: *Proc. of the 5th CIRP Int. Seminar on Computer-Aided Tolerancing*, 1997.

[5] Deck, J. F. and Dubowsky, S. On the limitations of predictions of the dynamic response of machines with clearance connections. *Journal of Mechanical Design* **116** (1994) 833–841.

[6] Erdman, Arthur, G. *Modern Kinematics: developments in the last fourty years.* (John Wiley and Sons, 1993).

[7] Goldberg, K., Halperin, D., Latombe, J., et al. (Eds.). *The Algorithmic Foundations of Robotics.* (A. K. Peters, Boston, MA, 1995).

[8] Gonzales-Palacios, M. and Angeles, J. *Cam Synthesis.* (Kluwer Academic Publishers, Dordrecht, Boston, London, 1993).

[9] Inui, M. and Miura, M. Configuration space based analysis of position uncertainties of parts in an assembly. in: *Proc. of the 4th CIRP Int. Seminar on Computer-Aided Tolerancing*, 1995.

[10] Joskowicz, L. and Sacks, E. Computational kinematics. *Artificial Intelligence* **51** (1991) 381–416. reprinted in [7].

[11] Joskowicz, L., Sacks, E., and Srinivasan, V. Kinematic tolerance analysis. *Computer-Aided Design* **29** (1997) 147–157. reprinted in [14].

[12] Latombe, J.-C. *Robot Motion Planning.* (Kluwer Academic Publishers, 1991).

[13] Latombe, J.-C. and Wilson, R. Assembly sequencing with toleranced parts. in: *Third ACM Symposium on Solid Modeling and Applications*, 1995.

[14] Laumond, J.-P. and Overmars, M. (Eds.). *Algorithms for Robotic Motion and Manipulation.* (A. K. Peters, Boston, MA, 1997).

[15] Litvin, F. L. *Gear Geometry and Applied Theory.* (Prentice Hall, New Jersey, 1994).

[16] Lozano-Pérez, T. Spatial planning: A configuration space approach. in: *IEEE Transactions on Computers*, volume C-32. IEEE Press, 1983.

[17] Parker, T. S. and Chua, L. O. *Practical Numerical Algorithms for Chaotic Systems.* (Springer-Verlag, New York, 1989).

[18] Requicha, A. A. G. Mathematical definition of tolerance specifications. *Manufacturing Review* **6** (1993).

[19] Sacks, E. and Bajaj, C. Sliced configuration spaces for curved planar bodies. *International Journal of Robotics Research* (1998). to appear.

[20] Sacks, E. and Joskowicz, L. Automated modeling and kinematic simulation of mechanisms. *Computer-Aided Design* **25** (1993) 106–118.

[21] Sacks, E. and Joskowicz, L. Computational kinematic analysis of higher pairs with multiple contacts. *Journal of Mechanical Design* **117** (1995) 269–277.

[22] Sacks, E. and Joskowicz, L. Dynamical simulation of planar systems with changing contacts using configuration spaces. Technical Report 97-008, Purdue University, 1997. To appear in *Journal of Mechanical Design.*

[23] Sacks, E. and Joskowicz, L. Parametric kinematic tolerance analysis of planar mechanisms. *Computer-Aided Design* **29** (1997) 333–342.

[24] Solomons, O., van Houten, F., and Kals, H. Current status of cat systems. in: *Proc. of the 5th CIRP Int. Seminar on Computer-Aided Tolerancing*, 1997.

[25] Voelcker, H. A current perspective on tolerancing and metrology. *Manufacturing Review* **6** (1993) 258–268.

[26] Whitney, D., Gilbert, O., and Jastrzebski, M. Representation of geometric variations using matrix transforms for statistical tolerance analysis. *Research in Engineering Design* **6** (1994).